Theoretical Chemistry Accounts (2020) 139:27
https://doi.org/10.1007/s00214-019-2530-2

REGULAR ARTICLE

Reactivity and stability of ion pairs, dimers and tetramers versus solvent polarity: S_NAr fluorination of 2-bromobenzonitrile with tetramethylammonium fluoride

Ellen V. Dalessandro[1] · Josefredo R. Pliego Jr.[1]

Received: 3 August 2019 / Accepted: 15 December 2019 / Published online: 18 January 2020
© Springer-Verlag GmbH Germany, part of Springer Nature 2020

Abstract
Anion–molecule reactions have a substantial solvent effect, which decreases with the solvent polarity. However, less solvation leads to the formation of ion pairs and higher aggregates that are usually less reactive. Consequently, theoretical determination of the best solvent for the reaction needs to consider all the species in equilibrium. In this report, we have investigated the wide range of solvent polarity in the S_NAr reaction of the tetramethylammonium fluoride (TMAF) with 2-bromobenzonitrile, as well as the formation of ion pairs, dimers and tetramers using molecular dynamics and density functional calculations with continuum solvation. Five solvents were considered: methanol, dimethylformamide, pyridine, tetrahydrofuran and benzene. The TMAF exists predominantly as free ions in methanol, as ion pairs in dimethylformamide and pyridine, and as tetramers in tetrahydrofuran and benzene. The reaction takes place through free ions in methanol, ion pairs in dimethylformamide, pyridine and tetrahydrofuran, and via dimer in benzene. The calculations suggest that dimethylformamide and pyridine are the best solvents for this reaction.

Keywords Ion pairing · Solvent effect · Nucleophilic fluorination · Aggregation · Counter-ion effect · Nucleophilic aromatic substitution · SNAr

1 Introduction

Reactions of ions with molecules, such as S_N2, E2 and S_NAr, can take place via the solvated ion in polar solvents. Increasing the solvation power (usually related to polarity) of the medium leads to increase in the activation free energy barrier. This is a classical view on this kind of reaction [1, 2]. Nevertheless, the counter-ion is also present in solution and formation of ion pairs takes place even in aqueous solution [3, 4]. With the decrease in the solvent polarity, dimers, trimers, tetramers and even higher aggregates can be formed [5]. Ionic reactions can also occur via these aggregates, although it is usually thought that single ions are more reactive [6]. Based on this view, aggregates can work like a buffer on the reactivity [7]. Indeed, reaction kinetics of the solvated ion becomes higher with the decrease in the solvent polarity and reaches the maximum value in the gas phase. Nevertheless, less polar solvents lead to formation of ion pairs and higher aggregates, which are usually less reactive. Consequently, there is an ideal solvation that produces the highest reactivity and it is worth to know how the reaction kinetics changes with the solvent polarity. Figure 1 shows a possible profile of the activation free energy versus solvation of the medium. In this profile, there is an ideal solvation window that leads to the highest kinetics.

In some situations, the solubility can be an additional factor that decides the best solvent. An example is the S_N2 reaction of cesium fluoride with alkyl halides or alkyl mesylates. Experimental data point out that while the reaction takes place in *tert*-butanol solvent, it is much less effective in methanol and acetonitrile solvents [8, 9]. Quantum chemistry and molecular dynamics calculations

“Festschrift in honor of Prof. Fernando R. Ornellas” Guest Edited by Adélia Justino Aguiar Aquino, Antonio Gustavo Sampaio de Oliveira Filho & Francisco Bolivar Correto Machado.

Electronic supplementary material The online version of this article (https://doi.org/10.1007/s00214-019-2530-2) contains supplementary material, which is available to authorized users.

✉ Josefredo R. Pliego Jr.
pliego@ufsj.edu.br

[1] Departamento de Ciências Naturais, Universidade Federal de São João del-Rei, São João del-Rei, MG 36301-160, Brazil

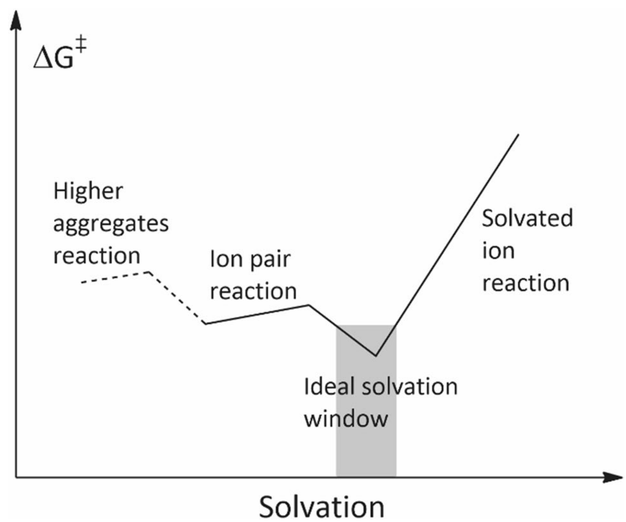

Fig. 1 General view of the solvent effect and formation of ion pairs and higher aggregates on the reactivity. Solvation refers to the sum of the solvation free energy of the pair of ions. See Ref. [7]

have pointed out that *tert*-butanol forms cyclic cluster in solution, which facilitates the solubility of CsF [10]. Furthermore, both the cesium counter-ion and *tert*-butanol molecules have a combined effect on the reactivity, participating of the transition state [10, 11]. The formation of ion pairs can also change the selectivity. As an example, the C- and O-alkylation of the phenoxide ion depends on the solvent and the formation of ion pairs [12–15].

Nucleophilic substitution reactions in aromatic rings, named S_NAr reactions, are very important transformations useful in synthetic chemistry. For a long time, these reactions have been thought to take place via a two-step mechanism, involving the formation of a Meisenheimer intermediate [16, 17]. This idea has dominated the literature of organic chemistry even considering that theoretical studies have long pointed out that a single-step mechanism is also observed [7, 18, 19]. However, a recent study combining experimental and theoretical methods by Jacobsen and co-workers has changed this view, supporting the idea that the concerted mechanism is the usual, whereas two-step mechanism occurs for more activated substrate [20]. In addition, an excellent and up-to-date review by Murphy and co-workers on this class of reactions has further contributed to a better perception on the main role of the concerted mechanism, which has also been named as cS_NAr reaction [21].

In recent years, the increased importance of organofluorine compounds has induced research toward the development of reagents and catalysts for more effective fluorination reactions [22–35]. An example is the tetramethylammonium fluoride. In 2008, theoretical calculations had shown that fluorination of 4-chlorobenzonitrile with $(CH_3)_4N^+F^-$, via S_NAr reaction with the ion pair, was feasible [7]. More recently, Sanford and co-workers have experimentally investigated this kind of reaction and they have confirmed the theoretical predictions that anhydrous tetramethylammonium fluoride is a viable reagent for aromatic ring fluorination [36]. Those authors have also observed that dimethylformamide is an adequate solvent for the reaction. Considering that dimers and tetramers could also be formed in solution phase, depending on the solvent polarity, it is worth to know the reactivity of these aggregates and the solvent effect considering several equilibria and reactivity. Thus, in this work we have investigated the reactivity of $(CH_3)_4N^+F^-$ ion pair with 2-bromobenzonitrile in different solvent polarities (Scheme 1), also including the formation of dimers and tetramers, via theoretical calculations.

2 Theoretical methods

2.1 Electronic structure calculations

The reaction shown in Scheme 1 involves ions, and the solvent effect on the geometry of minima and transition states is important. Thus, full geometry optimizations and harmonic frequency analysis were performed including the solvent effect. We have used the X3LYP functional [37] and the 6-31G(*d*) basis set for carbon and hydrogen, and 6-31 + G(*d*) basis set for fluorine, nitrogen and bromine. We have named this basis set as 6-31(+)G(*d*). The solvent effect was included through the SMD [38] method with *N*,*N*-dimethylformamide (DMF) solvent, using 240 tesserae for atom to obtain numerically more stable potential of mean force surface [39, 40].

Aimed to obtain reliable free energy in solution phase, we have used a composite method. Thus, for more accurate electronic energies, single point energy calculations were performed with the M08-HX functional [41] in conjunction

Scheme 1 Reaction investigated in this work

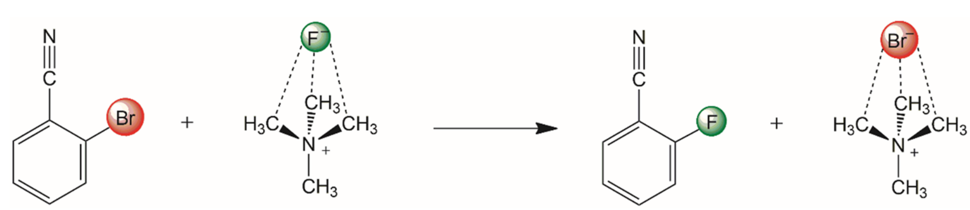

with the TZVPP basis set, augmented with sp diffuse functions on the fluorine, bromine and nitrogen atoms [42, 43]. The JANS = 2 option in the GAMESS program was used in the M08-HX computations to obtain better converged energies. Additional single point energy calculations in the gas phase and using the SMD model with the X3LYP/6-31(+)G(d) level of theory were performed to obtain the solvation free energy. The final free energy for each species in solution phase was calculated through the equation given below:

$$G_{\mathrm{sol}} = E_{\mathrm{el}} + G_{\mathrm{vrt}} + \Delta G_{\mathrm{solv}} + 1.89\ \mathrm{kcal\ mol^{-1}}$$

The first term in the right side is the electronic energy (M08-HX/TZVPP + diff), the second term is the vibrational, rotational and translational contributions to the free energy (SMD/X3LYP/6-31(+)G(d)), and the third term is the solvation free energy contribution calculated with the SMD model. The last term corresponds to the correction of the free energy from 1 atm standard state, adopted in the harmonic vibrational analysis, to 1 mol L^{-1} standard state, adequate for description of the solution phase processes. All the calculations were performed with the GAMESS program [44, 45].

2.2 Molecular dynamics calculations

The formation of a pair of ions in solution phase from single ions involves a substantial solvent effect, and usually cannot be described by a pure continuum solvation method. In this way, the use of molecular dynamic simulation can be useful for obtaining the structure of the solution. Thus, we have performed molecular dynamics simulation of the $(CH_3)_4N^+F^-$ species in solution of methanol and DMF solvents. For all the calculations, the OPLS-AA force-field was used [46]. Initially, the $(CH_3)_4N^+F^-$ species was placed in the center of a cubic simulation box with edge of 35 Å. In the following step, the solute in the box was solvated using a pre-equilibrated solvent box. The final number of solvent molecules included was 590 for methanol (edge of 34.3 Å after the simulation) and 265 for DMF (final edge of 32.4 Å).

The simulations were done with the velocity Verlet algorithm with a time step of 1 fs and constraining all of the bonds with the LINCS algorithm. A cutoff of 15 Å was applied for nonbonded interactions, and the PME method was used for the long-range electrostatic interactions. The NPT ensemble was adopted with the Berendsen thermostat, with a coupling time constant of 0.5 ps and temperature of 298 K. The Berendsen barostat was also utilized with a coupling time constant of 1.0 ps, compressibility of 5×10^{-5} and 1 atm of pressure. The simulations were performed with an equilibration run of 100 ps, followed by the production run of 1 ns. All the simulations were done with the GROMACS program [47], and the results were visualized with the VMD program [48].

3 Results and discussion

3.1 Structure of the solutions of tetramethyl ammonium fluoride

The structure of $(CH_3)_4N^+F^-$ ion pair in solution was probed by molecular dynamics simulation. Our goal was to determine whether the ion pair is stable for a long time in solution or rather the solvent is able to dissociate this species. We have used methanol and DMF as solvents because solvents with high dielectric constant are needed to separate ion pairs. Further, specific interactions such as hydrogen bonds are also very important. The results are presented in Fig. 2, which show the calculations of a long 1-ns simulation time. In the beginning of the simulation, the fluorine-to-nitrogen distance was 3.42 Å. After the 1 ns, this distance became 10.56 Å in methanol and only 3.56 Å in DMF. Thus, it is evident that methanol solvent is able to dissociate the ion pair, while the DMF solvent cannot. The fluoride ion exists as single solvated

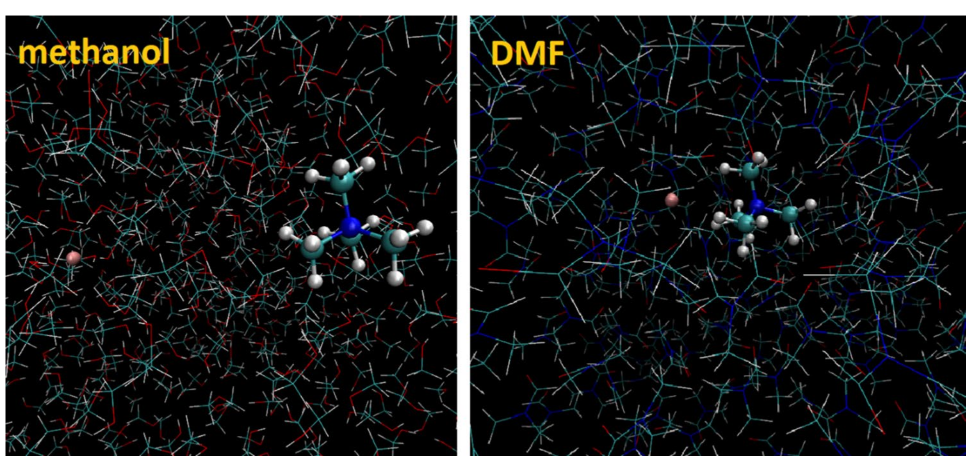

Fig. 2 Results of molecular dynamics simulation of $(CH_3)_4N^+F^-$ ion pair dissolved in methanol and DMF solvents at 298 K, after 1-ns simulation time

ion in methanol. In DMF, the fluoride ion remains in close contact with tetramethylammonium cation. It is worth to compare these results with the available experimental data. Thus, Sun and DiMagno have reported ^{1}H-^{19}F HOESY NMR spectroscopy studies of several trimethyl aryl ammonium fluoride salts and have concluded that these species exist as ion pairs in dimethyl sulfoxide solvent, which has very similar solvation properties of DMF [49]. This result is in agreement with our findings.

3.2 Reaction of the solvated fluoride ion in DMF and methanol

The structure of transition state for the reaction of the single fluoride ion with 2-bromobenzonitrile is presented in Fig. 3 (TS-F). The reaction takes place through a single step without formation of the classical Meisenheimer intermediate, usually postulated for this kind of reaction. The compact nature of the transition state, with C–F distance of 1.71 Å,

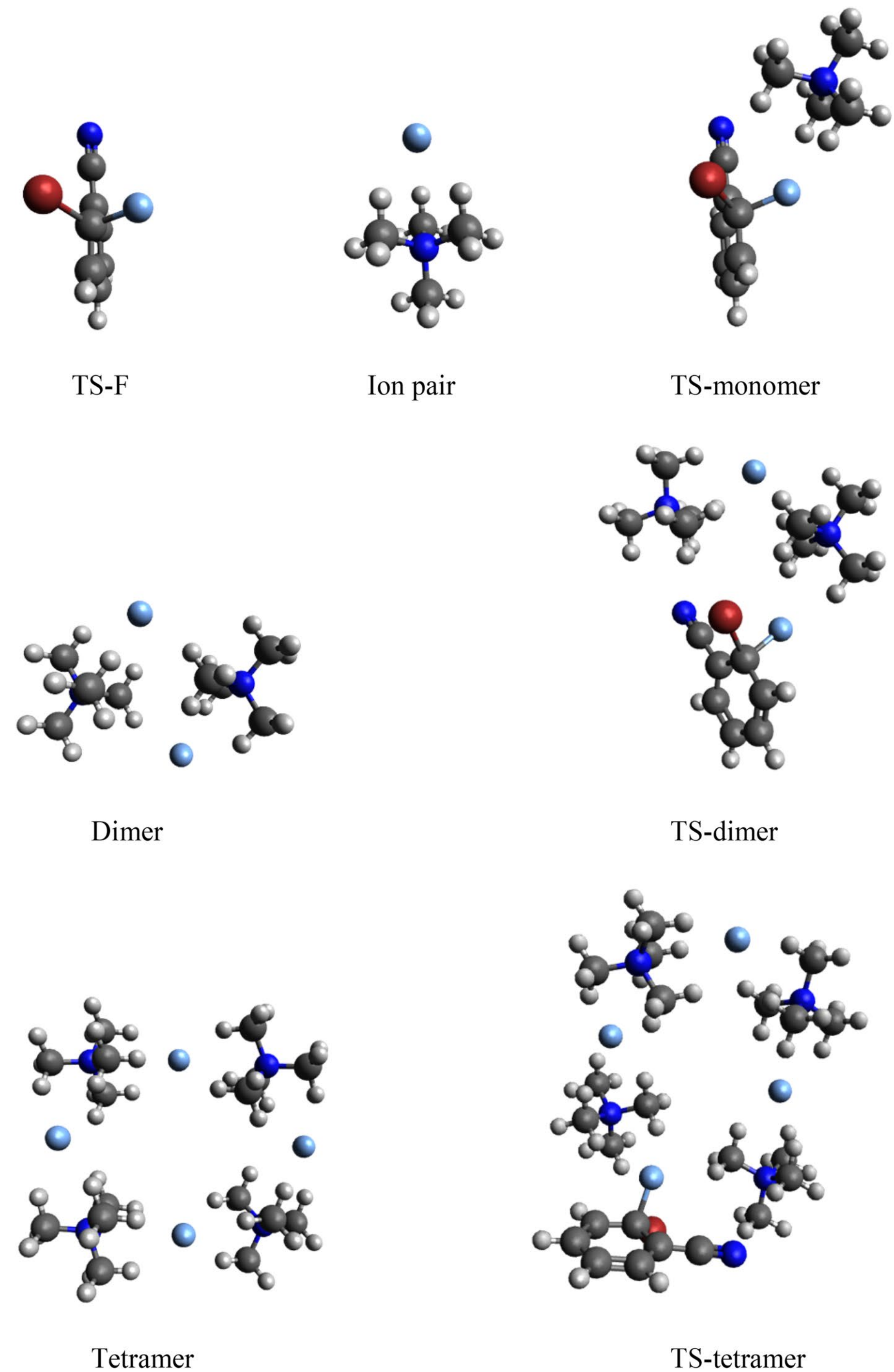

Fig. 3 Transition states and aggregates obtained at SMD/X3LYP/6-31(+)G(*d*) level of theory, DMF solvent

compared to C-F distance of 2.22 Å in aliphatic substrate [50], leads to a high solvent-induced barrier ($\Delta\Delta G_{solv}$) of 49 kcal mol^{-1} in methanol (Table 1). The final solution phase free energy barrier becomes 33.1 kcal mol^{-1}, which makes this reaction unfeasible in this solvent, in agreement with the experimental observations that this reaction was not reported in this solvent [36]. It is worth to say that the SMD model has a reasonable performance for ion-molecule reactions in methanol [51]. In addition, more reliable description of the solvation of the fluoride ion in methanol via hybrid discrete–continuum approach should make the barrier even higher [52].

The solvation free energy of the fluoride ion in methanol solution in the TATB compatible scale is − 109.2 kcal mol^{-1} [53], whereas in the solvents dimethyl sulfoxide and acetonitrile, which have similar solvation properties of DMF, the ΔG_{solv} values are in the range of − 88 to − 96 kcal mol^{-1} [54]. Thus, we could expect a meaningful difference in the activation free energy in methanol and DMF solvents. Nevertheless, this is not the case, because the calculated $\Delta G^{\ddagger}$ value in DMF is 33.3 kcal mol^{-1}, close to the 33.1 kcal mol^{-1} found in methanol solution. This is a flaw of the SMD model for description of single ion solvation in different solvents, especially polar aprotic, a problem recently reported [55].

Other evident flaws of SMD for ions in DMF are the prediction of dissociation of the $(CH_3)_4N^+F^-$ ion pair in DMF. Indeed, the calculations in Table 1 point out a positive free energy of 14.7 kcal mol^{-1} for the formation of the $(CH_3)_4N^+F^-$ ion pair. On the other hand, our results of molecular dynamics simulations predict that this ion pair is stable in the DMF solution. Experimental studies of solutions of fluoride ion with several ammonium cations show that these species exist as ion pairs in DMSO solution [49], providing more support for our molecular dynamic calculations. This limitation of the SMD (and continuum solvation models) for processes involving the formation of pair of ions from neutral species has been recently emphasized [51].

3.3 Reaction of the ion pair, dimer and tetramer in DMF

The transition state for the reaction of $(CH_3)_4N^+F^-$ ion pair with 2-bromobenzonitrile in DMF solvent is presented in Fig. 3. We can notice the close contact between the fluoride ion and its counter-ion. Because the ion pair is much less solvated than the pair of free ions (− 32 kcal mol^{-1} vs. − 148 kcal mol^{-1}), the solvent effect on the reaction is considerably smaller, only 12.2 kcal mol^{-1}. Consequently, the error is also smaller. As a rough estimation, considering that the error is 10%, the solvent-induced barrier for the ion pair reaction would have an uncertain of 1.2 kcal mol^{-1}, whereas in the case of the free fluoride ion reaction, the uncertain would reach 5 kcal mol^{-1}. Thus, the resulting free energy of activation in liquid phase is calculated to be 27.3 kcal mol^{-1}, indicating the feasibility of the reaction by this pathway. However, the formation of higher aggregates needs be evaluated.

The structure of the dimer is presented in Fig. 3. The gas phase contribution for its formation is − 19.1 kcal mol^{-1}. However, the solvent effect increases the free energy by 22.4 kcal mol^{-1}, leading to a positive free energy of 3.3 kcal mol^{-1}. Thus, the calculations predict that this species is present in equilibrium with the ion pair, although present in smaller concentrations. In the activation step, the variation

Table 1 Thermodynamics data for reaction and activation steps in DMF

Process	ΔE^a	ΔG_g^b	$\Delta\Delta G_{solv}^c$	ΔG_{sol}^d
F^- + *o*-NCPhBr → TS–F (in methanol)	− 21.5	− 16.0	49.1	33.1
$(CH_3)_4N^+ + F^- \rightarrow (CH_3)_4N^+F^-$	− 110.1	− 101.4	116.1	14.7
F^- + *o*-NCPhBr → TS–F	− 21.5	− 16.0	49.3	33.3
$(CH_3)_4N^+F^-$ + *o*-NCPhBr → TS-monomer	3.9	15.1	12.2	27.3
$(CH_3)_4N^+F^-$ + *o*-NCPhBr → $(CH_3)_4N^+Br^-$ + *o*-NCPhF	− 28.9	− 27.7	6.2	− 21.5
2 $(CH_3)_4N^+F^- \rightarrow [(CH_3)_4N^+F^-]_2$	− 27.3	− 19.1	22.4	3.3
$[(CH_3)_4N^+F^-]_2$ + *o*-NCPhBr → TS-dimer	− 4.7	8.6	18.7	27.4
$[(CH_3)_4N^+F^-]_2$ + *o*-NCPhBr → $(CH_3)_4N^+F^-(CH_3)_4N^+Br^-$ + *o*-NCPhF	− 33.1	− 31.5	8.1	− 23.4
2 $[(CH_3)_4N^+F^-]_2 \rightarrow [(CH_3)_4N^+F^-]_4$	− 52.8	− 41.4	36.3	− 5.1
$[(CH_3)_4N^+F^-]_4$ + *o*-NCPhBr → TS-tetramer	16.3	29.5	3.3	32.8
$[(CH_3)_4N^+F^-]_4$ + *o*-NCPhBr → $((CH_3)_4N^+F^-)_3(CH_3)_4N^+Br^-$ + *o*-NCPhF	− 25.4	− 22.0	2.4	− 19.6

Units in kcal mol^{-1}, 298 K, 1 mol L^{-1} standard state. Geometries and frequencies calculated at SMD/X3LYP/6-31(+)G(*d*) level

[a]Electronic energies obtained at M08-HX/TZVPP + diff level

[b]Gas phase free energies

[c]Solvent effect

[d]Solution phase free energy

of the electronic energy is negative by 4.7 kcal mol^{-1}, resulting in a gas phase free energy of 8.6 kcal mol^{-1}. The solvent effect further increases the solution phase free energy barrier to a value 27.4 kcal mol^{-1}. It is worth to notice that this dimer is as reactive as the ion pair and if the solvent effect is excluded, it is much more reactive. This unexpected result can be explained by an effective stabilization of the transition state by the two $N(CH_3)_4^+$ ions through a bridge structure (see Fig. 1). In spite of this interesting finding, the total free energy for the reaction through the dimer is 30.7 kcal mol^{-1}. Hence, this pathway does not compete with the ion pair reaction. The free energy profile in Fig. 4 gives a better view of these competing processes.

The other equilibrium considered in this study is the formation of the tetramer. This species has a plane structure, and its formation from two dimers has a very negative electronic energy of −52.8 kcal mol^{-1}. The gas phase free energy is −41.1 kcal mol^{-1}, and including the solvent effect raises the free energy by 36.3 kcal mol^{-1}, resulting in a liquid phase free energy of −5.1 kcal mol^{-1}. In the activation step, the electronic energy is 16.3 kcal mol^{-1}, leading to the gas phase activation free energy of 29.5 kcal mol^{-1}. The solvent effect is small, increasing the barrier by 3.3 kcal mol^{-1}. The final free energy barrier becomes 32.8 kcal mol^{-1}. Thus, the reactivity of the tetramer is substantially smaller than that of the monomer and dimer.

The overall free energy profile presented in Fig. 4 shows a general view of the reactivity of the different aggregates. Thus, analysis of this profile allows us to conclude that the reaction proceeds via ion pair (monomer) with a free energy barrier of 27.3 kcal mol^{-1}, making this reaction viable in the DMF solvent.

3.4 Free energy profile in benzene

The diagram in Fig. 1 points out methanol ($\varepsilon = 32.6$, polar protic) as a solvent in the right side leading to a low reactivity, whereas DMF ($\varepsilon = 37.2$, polar aprotic) is in the middle, with a better reactivity. The other extremum would be an apolar aprotic solvent such as benzene ($\varepsilon = 2.3$). Thus, we have computed the free energy profile of the reaction in benzene through single point SMD calculations using benzene as solvent (Fig. 5 and Table S1 in the supporting information). As expected, the free energy barrier for the monomer reaction is lower than in DMF as solvent, only 21.8 kcal mol^{-1}. In the case of the dimer reaction, the barrier is even smaller (19.1 kcal mol^{-1}). Nevertheless, this apolar solvent leads to strong aggregation of the monomers and the tetramer is 35 kcal mol^{-1} lower in free energy than in the monomer. These results indicate that all the $(CH_3)_4N^+F^-$ ion pairs are forming tetramers or ever higher aggregates not considered in this study. The reaction via tetramer has a free energy barrier of 31.8 kcal mol^{-1}, about 4.5 kcal mol^{-1} above the barrier in DMF via monomer. Further, this high barrier suggests that the reaction is inviable in this solvent. These findings are in qualitative agreement with Fig. 1.

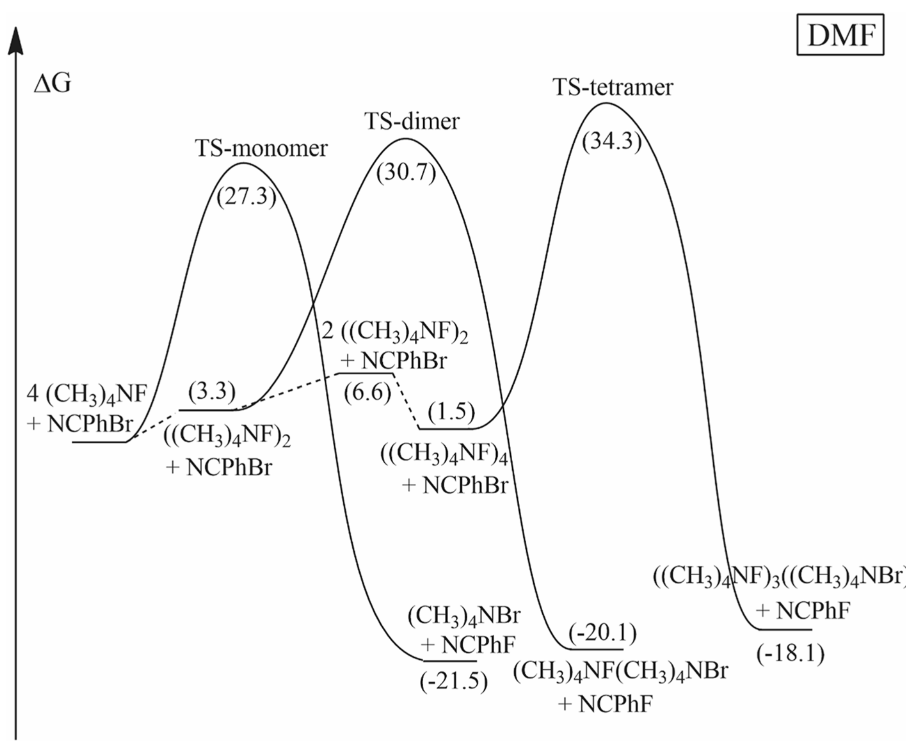

Fig. 4 Free energy profile of the reaction in Scheme 1 investigated in this work using DMF solvent. Units in kcal mol^{-1}, standard state at 1 mol L^{-1} and 298 K

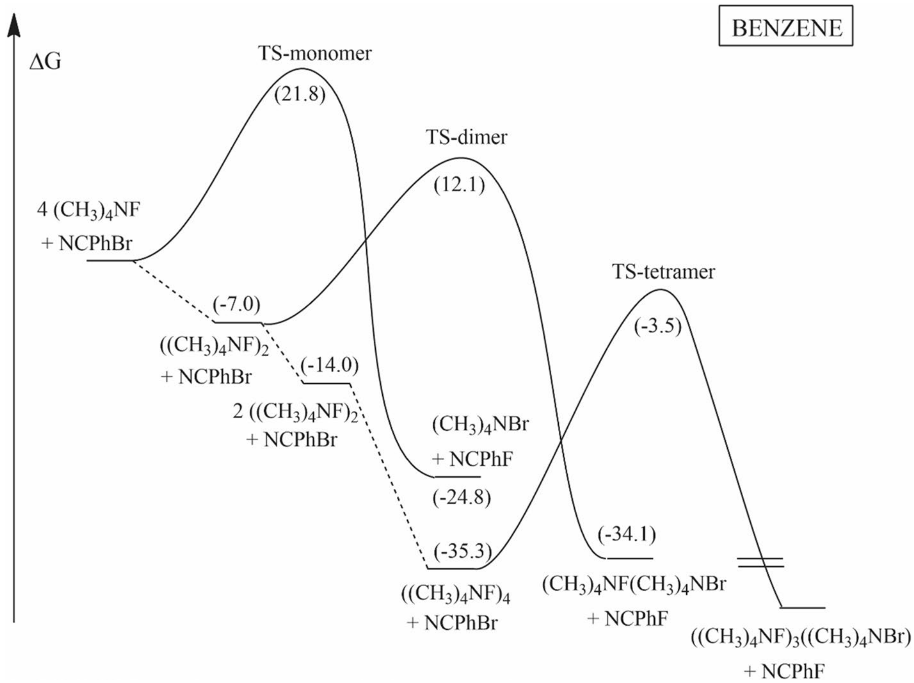

Fig. 5 Free energy profile of the reaction in Scheme 1 investigated in this work using benzene as solvent. Units in kcal mol^{-1}, standard state at 1 mol L^{-1} and 298 K

3.5 Free energy profile in pyridine and THF: the role of concentration

Based on Fig. 1, DMF should be a good solvent for the reaction because the monomers (ion pairs) are the dominant species in solution and the reaction proceeds through this step. Further, higher aggregates would not be formed in large extension. In the same time, DMF does not lead to high solvation of the fluoride ion like methanol solvent does. However, it would be interesting to test other less polar and aprotic solvents that could be even superior to DMF. We have chosen pyridine ($\varepsilon = 13.0$) and tetrahydrofuran (THF, $\varepsilon = 7.4$). Thus, we have performed single point SMD calculations on the optimized structures to obtain the free energy profile of the reaction in pyridine and THF solvents, presented in Fig. 6.

In pyridine solution, the formation of dimer should take place in a small extension, whereas the tetramer is more stable (− 3.1 kcal mol^{-1}). However, these small values of the free energy variation indicate that a full calculation of the equilibrium must be performed to determine the predominant species. In the case of the free energy barrier for the monomer reaction, the value of 26.7 kcal mol^{-1} is more favorable than in DMF as solvent. A similar trend is observed for THF as solvent, with a barrier for monomer reaction of only 25.8 kcal mol^{-1}. Nevertheless, in this case the tetramer is more stable, − 8.5 kcal mol^{-1}. For both of these solvents, we need to evaluate the equilibrium in the solution to determine the real kinetics based on the theoretical data. The equilibria involved are:

$$2\ \text{TMAF} \rightarrow (\text{TMAF})_2 \quad K_1$$

$$4\ \text{TMAF} \rightarrow (\text{TMAF})_4 \quad K_2$$

To determine the concentration of each species in equilibrium, we need to solve the equations:

$$K_1 = \frac{[(\text{TMAF})_2]}{[\text{TMAF}]^2}$$

$$K_2 = \frac{[(\text{TMAF})_4]}{[\text{TMAF}]^4}$$

$$[\text{TMAF}] + 2[(\text{TMAF})_2] + 4[(\text{TMAF})_4] = C_{\text{TMAF}}$$

where C_{TMAF} is the total or analytic concentration of the tetramethylammonium fluoride. The equilibrium constants K_1 and K_2 were obtained from the theoretical free energies. This set of equations was resolved for all the solvents investigated in this study, and the results are shown in Table 2, considering $C_{\text{TMAF}} = 0.40$ mol L^{-1} and the concentration of 2-bromobenzonitrile of 0.20 mol L^{-1}, a value close to the real synthetic conditions [36]. Once the concentrations were determined, we have used the activation barriers for each species to calculate the rate constants and the respective reaction rates at the beginning of the reaction at 298 K. Such analysis allows a more reliable evaluation on the true reaction kinetics and the role of each species.

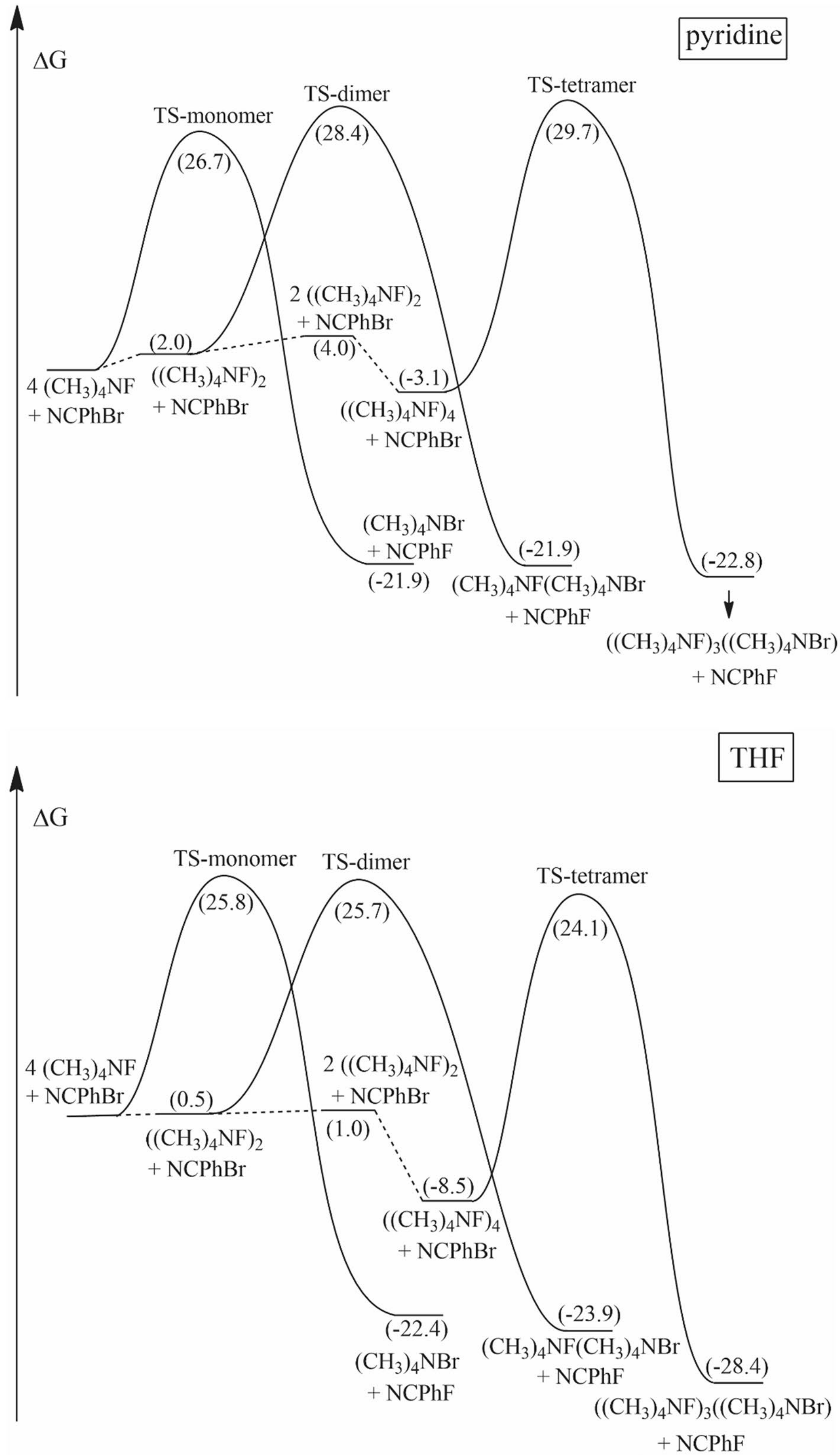

Fig. 6 Free energy profile of the reaction in Scheme 1 investigated in this work using pyridine and THF solvents. Units in kcal mol^{-1}, standard state at 1 mol L^{-1} and 298 K

The calculation of the reaction rate presented in Table 2 points out that for all the solvents investigated, including benzene, the reaction via the tetramer is less important. For this solvent, the reaction via dimer has the highest contribution. This unexpected finding for benzene solvent shows that in some systems a more detailed analysis of the kinetics, including concentration of the species, must be performed. In the case of THF, pyridine and DMF solvents, the

Table 2 Reaction kinetics in the beginning of the reaction

	Benzene	THF	Pyridine	DMF
[TMAF]	1.90E−07	0.0154	0.1371	0.3907
$[(TMAF)_2]$	4.89E−09	1.02E−04	6.41E−04	5.80E−04
$[(TMAF)_4]$	0.1000	0.0961	0.0663	0.0018
Rate (monomer)	2.42E−11	2.29E−09	4.46E−09	4.61E−09
Rate (dimer)	5.96E−11	4.17E−11	3.46E−11	5.78E−12
Rate (tetramer)	5.91E−13	1.47E−13	7.24E−14	2.02E−15
Rate (total)	8.43E−11	2.33E−09	4.49E−09	4.62E−09

Concentration in mol L^{-1}, and reaction rate in mol L^{-1} s^{-1}, 298 K

monomer reaction is the most important contribution for the total kinetics. Further, we can notice that the reactivity in DMF and pyridine is close, and even in THF it is slightly less reactive. There is a predominance of the monomer form in pyridine, whereas the tetramer predominates in THF. The reactivity in benzene is predicted to be 50 smaller than in DMF.

3.6 Comparison with experimental data

Sanford and co-workers have reported that anhydrous TMAF reacts with 2-bromobenzonitrile in the DMF solvent at 25 °C leading to 48% yield in 24 h [36]. Considering that the concentration of the 2-bromobenzonitrile substrate is 0.20 mol L^{-1} and that of the TMAF is 0.40 mol L^{-1}, a second-order kinetics leads to a rate constant of 2.2×10^{-5} L mol^{-1} s^{-1}. This rate constant corresponds to a free energy barrier of 23.8 kcal mol^{-1}. Sanford and co-workers have also reported the reaction at 80 °C, and in this case the same analysis leads to a free energy barrier of 25.6 kcal mol^{-1}. The value at 25 °C can be compared with our calculated barrier of 27.3 kcal mol^{-1} in DMF. The theoretical value is 3.5 kcal mol^{-1}, above the estimated experimental value. This is a reasonable agreement considering that the SMD model predicts too many positive barriers for anion–molecule reactions in polar aprotic solvents [55].

4 Conclusion

Theoretical calculations predict that tetramethylammonium fluoride forms ion pairs (monomers), dimers and tetramers in DMF, pyridine, THF and benzene. The monomer is the predominant species in DMF and pyridine solvents, whereas the tetramer is the main species in THF and benzene. In the polar and protic solvent methanol, TMAF exists as free ions. The S_NAr reaction with 2-bromobenzonitrile takes place through the monomer species in DMF, pyridine and THF, and via dimer in benzene. In methanol, the reaction involves the solvated fluoride ion. The theoretical analysis of the reactivity in these five solvents with a wide polarity and solvation range points out that DMF is the best solvent, although pyridine is predicted to be as effective as DMF. Our results also emphasize the importance of considering the formation of multiple species in solution phase when investigating ionic reactions, as well as to go beyond the free energy profile, taking into account the concentration of each species.

Acknowledgements The authors thank the agencies CNPq, FAPEMIG and CAPES for support.

Funding Funding was provided by Conselho Nacional de Desenvolvimento Científico e Tecnológico (Grant No. 303659/2018-1), Coordenação de Aperfeiçoamento de Pessoal de Nível Superior, Fundação de Amparo à Pesquisa do Estado de Minas Gerais.

References

1. Parker AJ (1969) Protic-dipolar aprotic solvent effects on rates of bimolecular reactions. Chem Rev 69:1
2. Pliego JR Jr (2009) First solvation shell effects on ionic chemical reactions: new insights for supramolecular catalysis. J Phys Chem B 113:505–510
3. van der Vegt NFA, Haldrup K, Roke S, Zheng J, Lund M, Bakker HJ (2016) Water-mediated ion pairing: occurrence and relevance. Chem Rev 116:7626–7641
4. Kohagen M, Pluhařová E, Mason PE, Jungwirth P (2015) Exploring ion-ion interactions in aqueous solutions by a combination of molecular dynamics and neutron scattering. J Phys Chem Lett 6:1563–1567
5. Marcus Y, Hefter G (2006) Ion pairing. Chem Rev 106:4585–4621
6. Alunni S, Pero A, Reichenbach G (1998) Reactivity of ions and ion pairs in the nucleophilic substitution reaction on methyl *p*-nitrobenzenesulfonate. J Chem Soc Perkin Trans 2:1747–1750
7. Pliego JR Jr, Pilo-Veloso D (2008) Effects of ion-pairing and hydration on the SNAr reaction of the f- with p -chlorobenzonitrile in aprotic solvents. Phys Chem Chem Phys 10:1118–1124
8. Kim DW, Jeong HJ, Lim ST, Sohn MH, Katzenellenbogen JA, Chi DY (2008) Facile nucleophilic fluorination reactions using tert-alcohols as a reaction medium: Significantly enhanced reactivity of alkali metal fluorides and improved selectivity. J Org Chem 73:957–962
9. Kim DW, Ahn DS, Oh YH, Lee S, Kil HS, Oh SJ, Lee SJ, Kim JS, Ryu JS, Moon DH, Chi DY (2006) A new class of SN2 reactions catalyzed by protic solvents: facile fluorination for isotopic labeling of diagnostic molecules. J Am Chem Soc 128:16394–16397
10. Pliego JR Jr (2017) Molecular dynamics and cluster-continuum insights on bulk alcohols effects on SN2 reactions of potassium and cesium fluorides with alkyl halides. J Mol Liq 237:157–163
11. Oh YH, Ahn DS, Chung SY, Jeon JH, Park SW, Oh SJ, Kim DW, Kil HS, Chi DY, Lee S (2007) Facile SN2 reaction in protic solvent: quantum chemical analysis. J Phys Chem A 111:10152–10161
12. Nogueira IC, Pliego JR Jr (2019) Counter-ion and solvent effects in the C- and O-alkylation of the phenoxide ion with allyl chloride. J Phys Org Chem 32:e3947
13. Berge A, Ugelstad J (1965) The effect of the solvent on the reactivity of sodium and potassium phenoxides in nucleophilic substitution reactions. Part II. relative reactivity of sodium and

potassion phenoxides in different aprotic solvents. Acta Chem Scand 19:742–750
14. Kornblum N, Seltzer R, Haberfield P (1963) Solvation as a factor in the alkylation of ambident anions: the importance of the dielectric factor. J Am Chem Soc 85:1148–1154
15. Kornblum N, Berrigan PJ, Le Noble WJ (1963) Solvation as a factor in the alkylation of ambident anions: the importance of the hydrogen bonding capacity of the solvent. J Am Chem Soc 85:1141–1147
16. François T (2013) Modern nucleophilic aromatic substitution. Wiley-VCH, Weinheim
17. Acevedo O, Jorgensen WL (2004) Solvent effects and mechanism for a nucleophilic aromatic substitution from QM/MM simulations. Org Lett 6:2881–2884
18. Glukhovtsev MN, Bach RD, Laiter S (1997) Single-step and multistep mechanisms of aromatic nucleophilic substitution of halobenzenes and halonitrobenzenes with halide anions: ab initio computational study. J Org Chem 62:4036–4046
19. Silva DR, Pliego JR (2019) How difficult are anion-molecule SNAr reactions of unactivated arenes in the gas phase, dimethyl sulfoxide, and methanol solvents? Struct Chem 30:75–83
20. Kwan EE, Zeng Y, Besser HA, Jacobsen EN (2018) Concerted nucleophilic aromatic substitutions. Nat Chem 10:917–923
21. Murphy J, Rohrbach S, Smith AJ, Pang JH, Poole DL, Tuttle T, Chiba S (2019) Concerted nucleophilic aromatic substitution reactions. Angew Chem Int Ed 58:16368–16388
22. Zhou Y, Wang J, Gu Z, Wang S, Zhu W, Aceña JL, Soloshonok VA, Izawa K, Liu H (2016) Next generation of fluorine-containing pharmaceuticals, compounds currently in phase II–III clinical trials of major pharmaceutical companies: new structural trends and therapeutic areas. Chem Rev 116:422–518
23. Yerien DE, Bonesi S, Postigo A (2016) Fluorination methods in drug discovery. Org Biomol Chem 14:8398–8427
24. Sather AC, Buchwald SL (2016) The evolution of Pd0/PdII-catalyzed aromatic fluorination. Acc Chem Res 49:2146–2157
25. Lee J-W, Oliveira MT, Jang HB, Lee S, Chi DY, Kim DW, Song CE (2016) Hydrogen-bond promoted nucleophilic fluorination: concept, mechanism and applications in positron emission tomography. Chem Soc Rev 45:4638–4650
26. Pupo G, Ibba F, Ascough DMH, Vicini AC, Ricci P, Christensen KE, Pfeifer L, Morphy JR, Brown JM, Paton RS, Gouverneur V (2018) Asymmetric nucleophilic fluorination under hydrogen bonding phase-transfer catalysis. Science 360:638–642
27. Jadhav VH, Choi W, Lee S-S, Lee S, Kim DW (2016) Bis-tert-alcohol-functionalized crown-6-Calix[4]arene: an organic promoter for nucleophilic fluorination. Chem Eur J 22:4515–4520
28. Pliego JR (2018) Potassium fluoride activation for the nucleophilic fluorination reaction using 18-crown-6, [2.2.2]-cryptand, pentaethylene glycol and comparison with the new hydro-crown scaffold: a theoretical analysis. Org Biomol Chem 16:3127–3137
29. Pliego JR (2018) Mechanism of nucleophilic fluorination promoted by bis-tert-alcohol-functionalized crown-6-calix[4]arene. Int J Quantum Chem 118:e25648
30. Pupo G, Vicini AC, Ascough DMH, Ibba F, Christensen KE, Thompson AL, Brown JM, Paton RS, Gouverneur V (2019) Hydrogen bonding phase-transfer catalysis with potassium fluoride: enantioselective synthesis of β-fluoroamines. J Am Chem Soc 141:2878–2883
31. Pfeifer L, Engle KM, Pidgeon GW, Sparkes HA, Thompson AL, Brown JM, Gouverneur V (2016) Hydrogen-bonded homoleptic fluoride-diarylurea complexes: structure, reactivity, and coordinating power. J Am Chem Soc 138:13314–13325
32. Engle KM, Pfeifer L, Pidgeon GW, Giuffredi GT, Thompson AL, Paton RS, Brown JM, Gouverneur V (2015) Coordination diversity in hydrogen-bonded homoleptic fluoride-alcohol complexes modulates reactivity. Chem Sci 6:5293–5302
33. Du X, Zhang H, Yao Y, Lu Y, Wang A, Wang Y, Li Z (2019) Fluorination of benzene with disubstituted N-fluoropyridinium salts in acetonitrile solution: a DFT study. Theor Chem Acc 138:28
34. Geng C, Du L, Liu F, Zhu R, Liu C (2015) Theoretical study on the mechanism of selective fluorination of aromatic compounds with Selectfluor. RSC Adv 5:33385–33391
35. Luo G, Luo Y, Qu J (2013) Direct nucleophilic trifluoromethylation using fluoroform: a theoretical mechanistic investigation and insight into the effect of alkali metal cations. New J Chem 37:10
36. Schimler SD, Ryan SJ, Bland DC, Anderson JE, Sanford MS (2015) Anhydrous tetramethylammonium fluoride for room-temperature SNAr fluorination. J Org Chem 80:12137–12145
37. Xu X, Zhang Q, Muller RP, Goddard WA III (2005) An extended hybrid density functional (X3LYP) with improved descriptions of nonbond interactions and thermodynamic properties of molecular systems. J Chem Phys 122:014105–014114
38. Marenich AV, Cramer CJ, Truhlar DG (2009) Universal solvation model based on solute electron density and on a continuum model of the solvent defined by the bulk dielectric constant and atomic surface tensions. J Phys Chem B 113:6378–6396
39. Su P, Li H (2009) Continuous and smooth potential energy surface for conductorlike screening solvation model using fixed points with variable areas. J Chem Phys 130:074109–074113
40. Silva CM, Dias IC, Pliego JR (2015) The role of ammonia oxide in the reaction of hydroxylamine with carboxylic esters. Org Biomol Chem 13:6217–6224
41. Zhao Y, Truhlar DG (2008) Exploring the limit of accuracy of the global hybrid meta density functional for main-group thermochemistry, kinetics, and noncovalent interactions. J Chem Theory Comput 4:1849–1868
42. Zheng JJ, Xu XF, Truhlar DG (2011) Minimally augmented Karlsruhe basis sets. Theor Chem Acc 128:295–305
43. Weigend F, Ahlrichs R (2005) Balanced basis sets of split valence, triple zeta valence and quadruple zeta valence quality for H to Rn: design and assessment of accuracy. Phys Chem Chem Phys 7:3297–3305
44. Gordon MS, Schmidt MW (2005) Chapter 41:advances in electronic structure theory: GAMESS a decade later. In: Dykstra CE, Frenking G, Kim KS, Scuseria GE (eds) Theory and applications of computational chemistry. Elsevier, Amsterdam, pp 1167–1189. https://doi.org/10.1016/B978-044451719-7/50084-6
45. Schmidt MW, Baldridge KK, Boatz JA, Elbert ST, Gordon MS, Jensen JH, Koseki S, Matsunaga N, Nguyen KA, Su S, Windus TL, Dupuis M, Montgomery JA Jr (1993) General atomic and molecular electronic structure system. J Comput Chem 14:1347–1363
46. Jorgensen WL, Maxwell DS, Tirado-Rives J (1996) Development and testing of the OPLS all-atom force field on conformational energetics and properties of organic liquids. J Am Chem Soc 118:11225–11236
47. Van Der Spoel D, Lindahl E, Hess B, Groenhof G, Mark AE, Berendsen HJC (2005) GROMACS: fast, flexible, and free. J Comput Chem 26:1701–1718
48. Humphrey W, Dalke A, Schulten K (1996) VMD: Visual molecular dynamics. J Mol Graphics 14:33–38
49. Su HR, Wang B, DiMagno SG (2008) Ion pairing of "weakly coordinated" fluoride salts. Chim Oggi 26:4–6
50. Pliego JR Jr, Piló-Veloso D (2007) Chemoselective nucleophilic fluorination induced by selective solvation of the SN2 transition state. J Phys Chem B 111:1752–1758
51. Silva NM, Deglmann P, Pliego JR (2016) CMIRS solvation model for methanol: parametrization, testing, and comparison with SMD, SM8, and COSMO-RS. J Phys Chem B 120:12660–12668
52. Pliego JR Jr., Riveros JM (2019) Hybrid discrete-continuum solvation methods. Wiley Interdiscip Rev Comput Mol Sci 2019:1440

53. Pliego JR, Miguel ELM (2013) Absolute single-ion solvation free energy scale in methanol determined by the lithium cluster-continuum approach. J Phys Chem B 117:5129–5135
54. Carvalho NF, Pliego JR (2015) Cluster-continuum quasichemical theory calculation of the lithium ion solvation in water, acetonitrile and dimethyl sulfoxide: an absolute single-ion solvation free energy scale. Phys Chem Chem Phys 17:26745–26755
55. Miguel ELM, Santos CIL, Silva CM, Pliego JR Jr (2016) How accurate is the SMD model for predicting free energy barriers for nucleophilic substitution reactions in polar protic and dipolar aprotic solvents? J Brazil Chem Soc 27:2055–2061

Publisher's Note Springer Nature remains neutral with regard to jurisdictional claims in published maps and institutional affiliations.